

# Numerical Study of the Influence of the Number of Stator and Rotor Blades on the Cavitation Behavior of a Kaplan Hydraulic Turbine

Aymen Mefti<sup>1</sup>, Ibrahim Ayad<sup>2\*</sup>, Mahfoudh Cerdoun<sup>1</sup>, Smail Khalfallah<sup>1</sup> and  
Djahida Boucetta<sup>3</sup>

<sup>1</sup> Laboratory of Turbomachinery, Polytechnic Military School (EMP), BP 17, Bordj El Bahri, Algiers, 16046, Algeria

<sup>2</sup> Aero-Hydrodynamic Naval Laboratory (LAHN), Faculty of Mechanical Engineering, University of Science and Technology of Oran Mohamed Boudiaf (USTO-MB), 31000 Oran, Algeria

\* E-Mail: ibrahim.ayad@yahoo.fr

<sup>3</sup> Maritime Technology Division, Ghent University, Technologiepark 60, 9052 Ghent, Belgium

## ABSTRACT

The understanding and accurate prediction of the flow behavior in a Kaplan turbine are important to the design work enhancing the turbine performance including the elongation of the operation life span and the improvement of turbine efficiency. The present work concerns a stationary numerical investigation of an axial hydraulic turbine of the Kaplan type in order to study the influence of the numbers of stator and rotor blades on the flow behavior related to cavitation through the commercial code ANSYS CFX. The operating conditions of this axial turbine, similar to those encountered in a previous experiment, made it possible both to validate the numerical model and to identify the nominal operating regime. In addition, variations in the numbers of stator and rotor blades have shown observations regarding the influence of the numbers of stator and rotor blades on the cavitation phenomenon.

**Keywords:** turbine, Kaplan, CFD, hydrodynamic performance, number of stator and rotor blades, cavitation phenomenon

## 1 INTRODUCTION

Cavitation is a significant phenomenon observed in several topics related to liquid transportation. It is a physical event that causes vapor bubbles to form in a fluid flow. When fluid velocity increases, pressure decreases, lowering the boiling point of the fluid until it reaches the surrounding temperature. Cold boiling occurs when the local fluid pressure falls below the saturation pressure, producing vapor or vapor-filled bubbles. A cavity of this type has two phases: formation and growth. These vapor bubbles implode due to an increase in fluid local pressure, with no external energy input. The cavitation bubbles collapsing generate impingement jets with a high energy density, eroding the adjacent solid surface [1]. Cavitation in hydraulic machinery causes severe material damage, noise, blade erosion, and other problems, resulting in a decrease in operation quality and life. It causes flow obstruction, erodes the flow passage, and causes violent pressure vibrations that necessitate costly repair stops or turbine replacements [2]. This is a serious problem for the designers and operators of large axial turbines. Cavitation initiation and development are influenced by runner design, as well as unstable operating conditions and machine level setting. Cavitation limitations limit the turbine's maximum output at maximum operating conditions.

Due to its low head and wide range of operating conditions, the Kaplan turbine is widely used in hydropower plants with good hydrodynamic and energy characteristics. In this context, the manufacturers of Kaplan turbines have forced themselves to increase their yields and their powers and have focused on improving the various components of these. Understanding the complex flows, rotor- stator interactions and their effects on the aerodynamic performance inside these turbines will certainly improve their performance. Luis et al. [3] showed the usefulness of numerical simulations on a scale model of a Kaplan turbine, using the commercial software CFX, based on a tetrahedral mesh, in order to evaluate three turbulence models namely,  $k-\epsilon$ ,  $k-\omega$  and the one-equation model KE1E. Gehrler et al. [4] Showed that the domain decomposition and the use of stage-type interfaces predicted the hydrodynamic performances in agreement with the experimental results, and that close to the operating condition associated with the optimal efficiency, but the deviation increases away from this optimal point. Santos et al. [5] carried out simulations of a bulb turbine for separate domains and for a complete machine, in order to validate the impeller diameter proposed by the manufacturer for the real installation. The representation of the pressure field and the velocity vectors in the inlet channel indicates that the flow in this part is stable and regular. They found that there is almost no difference when simulating a complete machine versus separate domains. Works centered on the flow in a complete machine have been approached by Begnigni and Jaberg [6]. To reduce the size of the computational domains and to reduce the time of the

simulations, the periodicity of the passage of the propeller and the distributor can be used. Indeed, the calculation domains of the distributor and the propeller are composed of single and periodic passages. Edwin [7] presents the numerical modeling and analysis of the flow in a single passage of the propeller of an axial hydraulic turbine of the propeller type (non-steerable rotor blade) with and without blade tip clearance. Simulation results for a Kaplan turbine including the blade tip clearance were presented by Nilsson et al. [8] who analyzed stationary and periodic flows in a quarter of the propeller domain of this turbine, having four blades and 24 directors and among the phenomena studied by the authors, the blade tip vortex which was the most detailed. As in any hydraulic machinery, cavitation can also occur in Kaplan turbine at different operating conditions. Ayli [9] observes cavitation at the blade suction side. Grekula et al. [10] conduct an experimental study which allows him to observe cavitation at the blade hub fillet and blade surface near the hub. Sheet cavities also cause flow separation at the blade leading edge due to mismatched angle of attack. Reentrant jets, bubble formation, and cavitating vortices are also observed at the leading edge in partial load conditions. Several types of cavities can occur in Kaplan turbines which require better understanding of the flow pattern to avoid such a serious problem. To help better understand the phenomena occurring in hydraulic turbines, the present study applies directly to a Kaplan-type turbine (Figure 1) used for low head heights of about 12 m to 60 m and for a wide range of debits.

A numerical investigation of the flow dynamics in this turbine, using stationary numerical simulations (CFD), is possible. The main objective of this investigation is to analyze the structures characterizing the hydrodynamic behavior of the flows through the different components of this turbine by varying the number of stator and rotor blades and to see the behavior of the flow vis-à-vis the phenomenon of cavitation. A general conclusion of the present study which will include all the relevant results obtained will be the end of this manuscript, with a proposal of some perspectives allowing the improvement of the results obtained and the exploitation of other operating fields of this turbine in the purpose of improving the understanding of the phenomena recorded and studied.



**Figure 1.** A real model of the Kaplan water turbine.

## 2 NUMERICAL SIMULATIONS

The turbine is divided into three domains: the distributor, the propeller, and the diffuser as shown in Figure 2a. These subdomains are connected by interfaces: stage, to predict aerodynamic performance and with a GGI-type node connection method general grid interface. The commercial code CFX was used to perform the simulations considering: the turbulence model  $k-\omega$  SST with an automatic wall function. The boundary conditions are as follows: total pressure at the inlet, mass flow at the outlet, flux conservation at the periodic interfaces, and condition of non-slip on the solid walls.

### 2.1 Model Evaluation

In this study, the meshing of each of the rotor and stator components was carried out separately by using the "TurboGrid" software of the ANSYS CFX commercial software. The resulting mesh is shown in Figure 2b while Figure 2c presents the mesh of the diffuser which was performed through the use of the "Gambit" code. The number of elements and nodes in this domain are 966403 and 1029542, respectively. The number of elements and nodes in this domain are as follows: distributor (230656, 250848), propeller (627247, 662822), and diffuser (108500 115872).

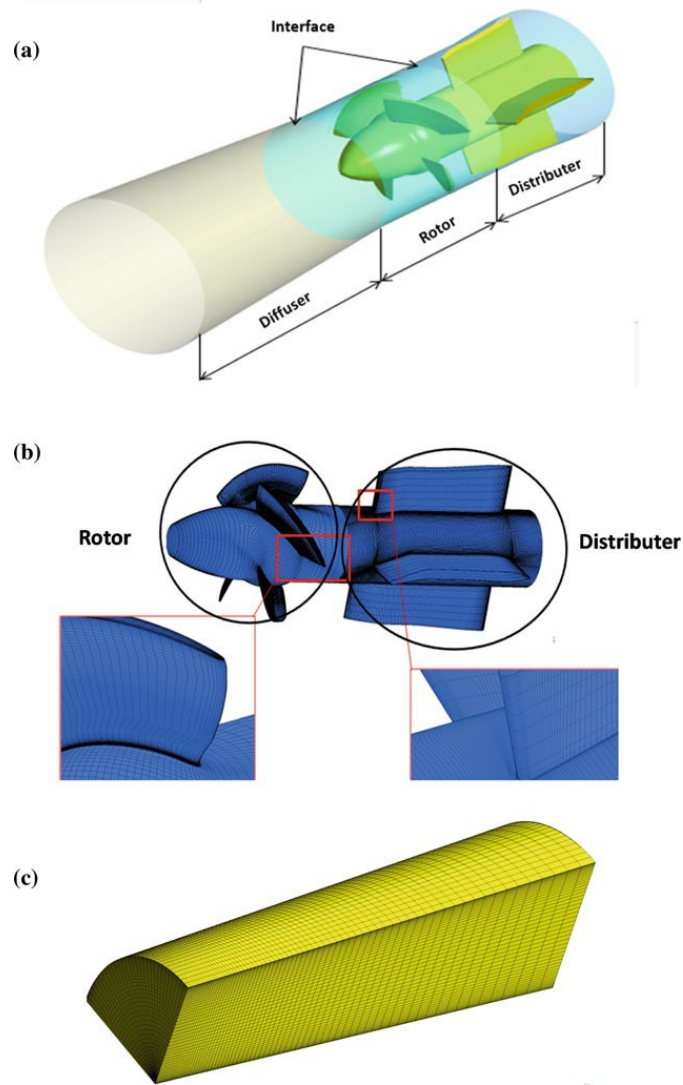


**Figure 2.** (a) Calculation domain. (b) Refinement zone expansions. (c) Diffuser mesh.

## 2.2 Mesh Dependency

Given the large quantity of simulations to be performed, it is important to reduce the calculation times as much as possible without reducing the quality of the results. The calculated power for different sizes of the mesh made it possible to retain a total mesh size of 1,029,542 nodes to perform our calculations (Figure 3).

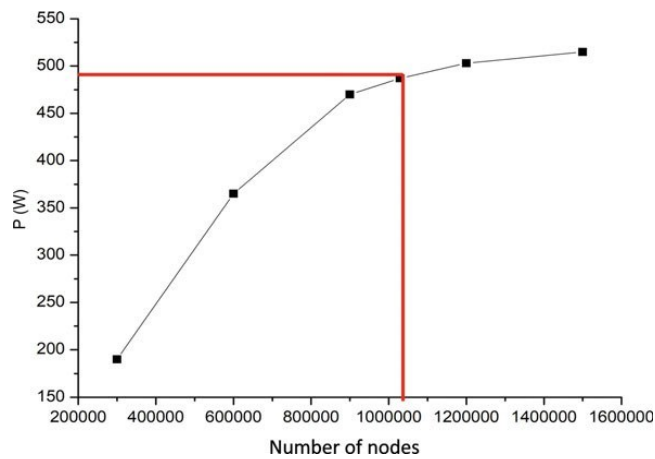


**Figure 3.** Effect of mesh sizes on power.

### 2.3 Mesh of the Different Configurations of Stator and Rotor Blades

In hydraulic turbines, the number of directional blades of the distributor can be different from the number of blades of the propeller for several reasons. When the pitch of the impeller blades is different from the pitch of the guide vanes, it is preferable to digitally simulate the two complete domains (distributor–impeller). However, the disadvantage is still the high need for computing resources and data storage. It is therefore necessary to reduce the problem by dividing the distributor and the impeller into periodic sections. If the blades of the impeller and the guide vanes of the distributor have a different pitch,  $N$  passages on one side and  $M$  passages on the other side can also be simulated, by making the passage of the first domain equal to  $360/N$  and the other domain is equal  $360/M$ . Figure 4a shows the configuration for a number of stator vanes  $N_S = 5$  and a number of rotor vanes  $N_R = 4$  (the first pass is equal to  $360/5 = 72^\circ$ , and the second pass is equal to  $360/4 = 90^\circ$ ). The mesh of the last domain, which is the diffuser, has been modified for each configuration of number of rotor and stator blades so that the passage section depends on the passage section of the rotor, by making the interface area of the passages of two sides coincides perfectly ( $360/N_R$ ). Figure 4b shows the different passage sections of the diffuser part for each number of rotor blades  $N_R$ .

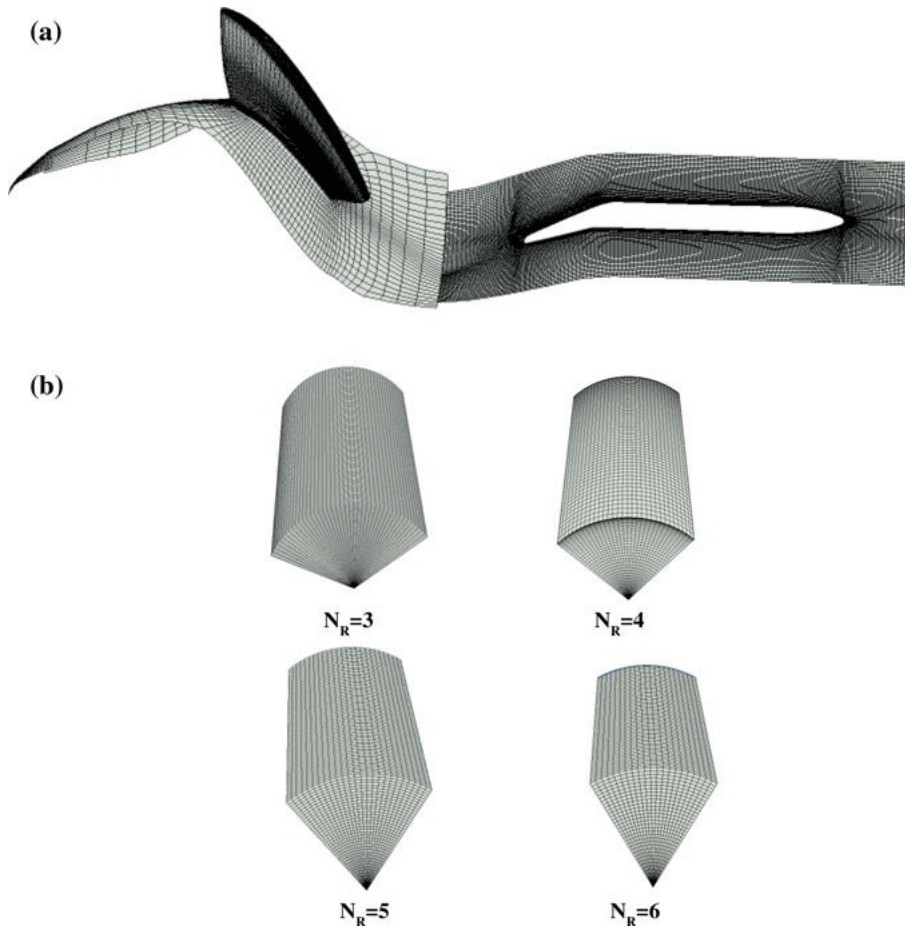


**Figure 4.** (a) Periodic passage for a number of stator blades  $N_S = 5$  and number of rotor blades  $N_R = 4$ . (b) Different passage sections of the diffuser part.

### 2.4 Boundary Conditions

After modeling the Kaplan turbine and discretizing the computational domains, the next step is to define the general calculation conditions which are as follows: simulation domain (one inter-blading channel (periodicity condition)), fluid (water), edge- input condition (total pressure = 128,511 Pa), edge-output condition (mass flow), heat transfer (isothermal, 318 K), turbulence model ( $k-\omega$  SST), interfaces (stage), averaged residual ( $10^{-6}$ ), advection scheme (upwind).

## 2.5 Wall Condition

This is the default condition for all boundaries of the computational domain. For the first mesh of the periodic domain, shown in Figure 5, we estimated an initial distance between the solid walls and the first layer of nodes ( $\Delta y$ ). This distance varies depending on the value of the variable  $y^+$  required by the turbulence model to be used in a numerical calculation. Since the turbulence model used is  $k-\omega$  SST based on a wall law which makes it possible to establish a distance  $y^+$  relatively less than 100, we have therefore estimated this distance  $\Delta y$  around the blade based on a target value  $y^+=1$ , and at nominal operating conditions ( $N = 2000$  rpm and  $Q = 36$  kg/s).

*For the Distributor:*  $C_{av} = 78.36$  mm,  $V = 4.7$  m/s,  $\rho = 997$  kg/s and  $\mu = 8.89 \cdot 10^{-4}$  kg/ms, so  $Re = (\rho C_{av} V) / \mu = 413,033.88$ , for a target value of  $y^+ = 1$ , the initial distance  $\Delta y = 0.0047$  mm.

*For the Rotor:*  $C_{av} = 52.2$ mm,  $V = 5.4$  m/s,  $\rho = 997$  kg/s and  $\mu = 8.89 \cdot 10^{-4}$  kg/ms, so  $Re = (\rho C_{av} V) / \mu = 315,743.62$ , for a target value of  $y^+ = 1$ , the initial distance  $\Delta y = 0.004$  mm.

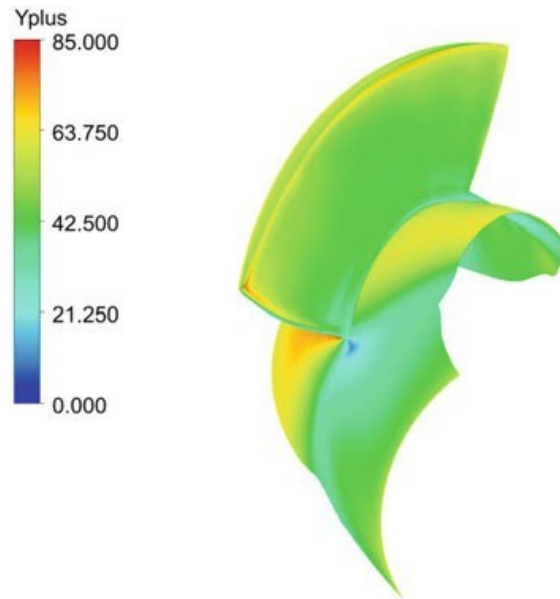


Figure 5. Distribution of  $y^+$  on the walls of the blades and on the propeller hub.

## 3 RESULTS AND DISCUSSION

### 3.1 Model Validation

It is important to ensure beforehand that the model adapted for CFD calculations is adequate. Indeed, numerical simulations were carried out for the case of the number of stator blades fixed at 4 and the number of rotor blades fixed at 4. The results obtained are compared with some experimental results available for the same model. Figure 6a and 6b, respectively, illustrate measured and calculated power and efficiency as a function of rotational speed for different mass flow rates. It is noticed that the shapes of the predicted efficiency and power curves are in good agreement with the measured curves, which proves that the adopted model and the chosen parameters are satisfactory.

It should be noticed that both Figure 6a and 6b give the nominal point at the same operating range, whether for numerical or experimental results. The speed of 2000 rpm with a flow rate of 36 kg/s defines a nominal operating point for this Kaplan turbine (the maximum efficiency is around 52.67%, and the maximum power delivered is around 490 W). It is also noted that outside the adaptation regime (nominal), there is a drop in efficiency and power. This decrease can be explained by the increase in losses caused by secondary flows, friction, and seepage flow.

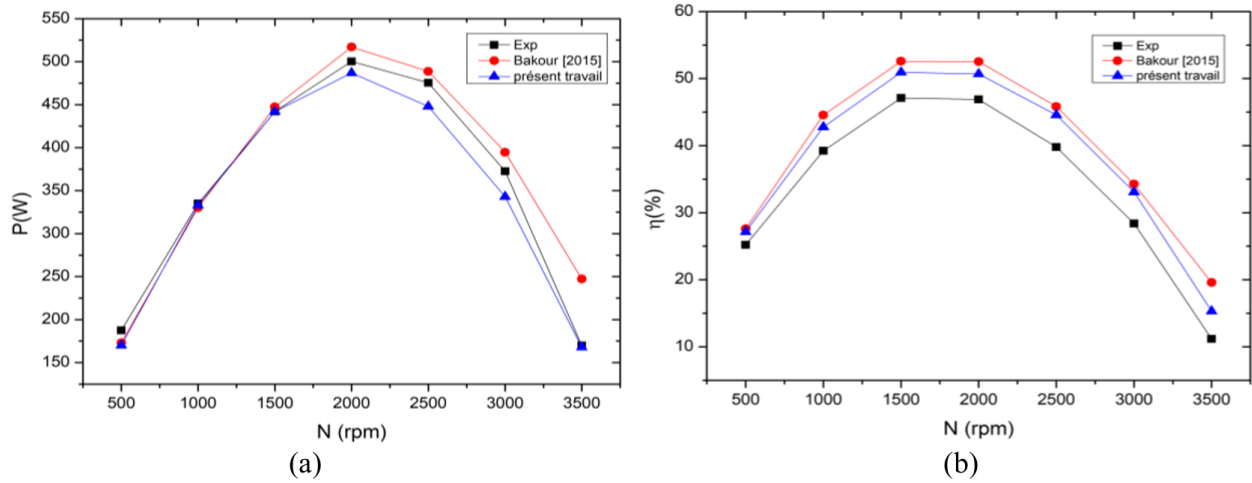


Figure 6. (a) Evolution of power according to the speed of rotation. (b) Evolution of efficiency as a function of rotation speed.

### 3.2 Cavitating Flow of the Kaplan Turbine

We present in this section the results of the simulations of the cavitating flow, in which we will focus on the effects of the number of stator blades  $N_S$  and the number of rotor blades  $N_R$  on the formation of cavitation bubbles. The general calculation conditions are as follows: saturated vapor pressure ( $P_V = 3576$  Pa), temperature (isothermal 297 K), cavitation model (Rayleigh–Plesset), fluid (two-phase mixing), bubble diameter ( $2 \cdot 10^{-6}$ ).

#### 3.2.1 Effect of Number of Stator Blades $N_S$

In this section, the effect of the parameters of number of stator vanes  $N_S$  on the establishment of the cavities on the rotor blade is studied. Indeed, four configurations of ( $N_S = 3$ ,  $N_S = 4$ ,  $N_S = 5$ , and  $N_S = 6$ ) were tested at the nominal operating point (rotation speed 2000 rpm and  $Q = 35$  kg/s) but keeping each time the number of rotor blades,  $N_R$  fixed (3, 4, 5, and 6). Figure 7 is an illustration of the distribution of the vapor volume fraction on the impeller blade for the different configurations.

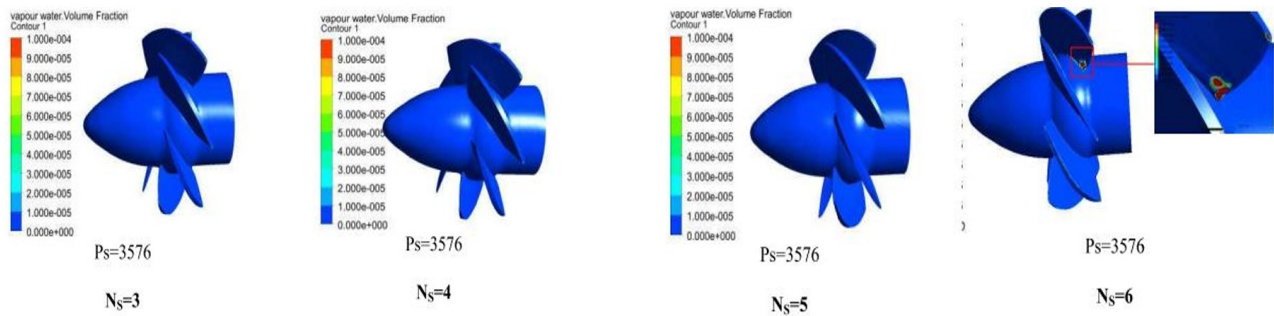


Figure 7. Distribution of the volume fraction of water vapor.

It is noticed that there is almost no formation of cavitation bubbles for all the configurations. Nevertheless, the appearance of a small cavity zone is observed in the clearance between the tip of the blade and the hub, in the case where the number of stator blades is equal to 5 and 6 and, moreover, on the extrados surface of the blade side of the leading edge precisely for  $N_S = 6$ . This is due to the strong acceleration of the streamlines at this location which results in a drop in the static pressure which is equal to or below the saturation vapor pressure  $P_V = 3576$ . In addition, we note that the coefficient which describes the cavitation (Thomas coefficient)  $\sigma = NSPH/H$  decreases linearly when the number of stator vanes  $N_S$  is increased (Figure 8), showing of course that we are approaching the conditions of bad hydrodynamic operation of the turbine with respect to the cavity phenomenon.

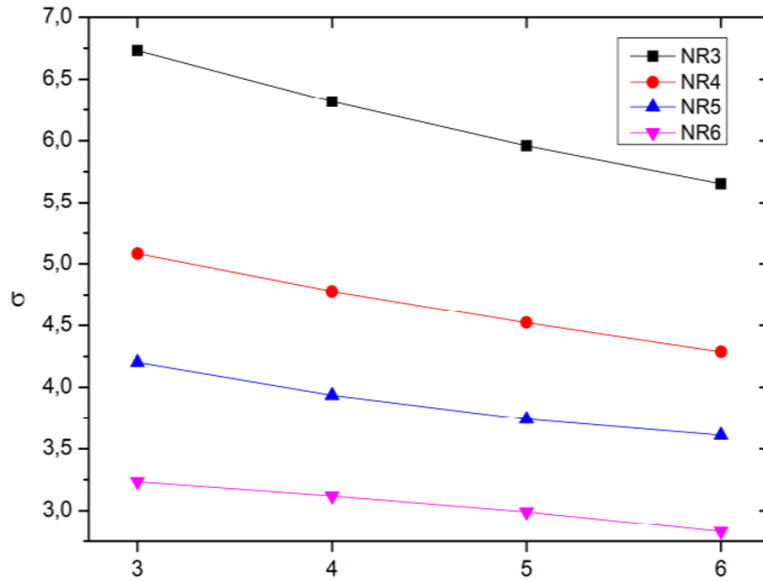


Figure 8. Variation of the Thomas coefficient as a function of the number of stator blades.

### 3.2.2 Effect of Number of Rotor Blades NR

In this part, we are interested in observing and analyzing the behavior of the flow vis-à-vis the cavitation phenomenon while highlighting the effect of the number of rotor blades. Indeed, four configurations (NR =3, NR =4, NR =5, and NR =6) were tested for a fixed rotation speed of 2000 rpm and a flow rate of  $Q = 36$  kg/s while keeping each time a fixed number of stator blades (3, 4, 5, and 6). It is noted that the effect of increasing the number of rotor blades and for the case of NS=6, the flow undergoes a great depression on the extrados side of the rotor blade. We can moreover note that when the number of rotor blades NR increases, there is an increase in the volume produced by pockets of water synonymous with the volume occupied by cavitation.

### 3.2.3 Comparison of Turbine Performance Between Cavitating and Non-cavitating Flow

Table1 includes the results in terms of the power of the turbine in non-cavitating and cavitating flow for a fixed speed of 2000 rpm. This table shows a slight drop in the hydrodynamic power of the turbine following the formation of the pockets of cavity. The magnitude of this decrease is a function of the size of the steam pocket as well as its extension. Therefore, the addition of stator and rotor blades does not have a large effect on the operation of the turbine, which consolidates the idea of modifying the blades to have more power.

Table 1 Turbine performance between cavitating (Cav) and non-cavitating (No Cav) flow

	No Cav				Cav		
	P(W)	P(W)	NSPH		P(W)	P(W)	NSPH
NS3–NR3	327.478	327.125	12.658	NS5–NR3	374	373.366	12.63
NS3–NR4	455	454.781	12.546	NS5–NR4	515.205	515.169	12.474
NS3–NR5	548	547.425	12.659	NS5–NR5	615.53	615.417	12.478
NS3–NR6	659	658.571	12.547	NS5–NR6	733	732.539	12.631
NS4–NR3	351.87	351.863	12.648	NS6–NR3	392	391.61	12.605
NS4–NR3	487	583.69	12.511	NS6–NR4	539.96	539.626	12.431
NS4–NR3	583.934	583.69	12.516	NS6–NR5	644	643.604	12.612
NS4–NR3	698	698.054	12.648	NS6–NR6	763.105	761.926	12.433

## 4 CONCLUSION

The general objective of this study was to numerically investigate the influence of the number of stator and rotor blades on the flow behavior related to cavitation of a Kaplan-type hydraulic turbine. More specifically, the project consisted of an investigation in a steady flow regime without and with the implication of the cavitation phenomenon. The first section focused on the reliability of the CFD tool.

As a first conclusion, the CFD results showed excellent agreement between the numerical results and the available experimental data. The second objective of this study was to study and analyze the behavior of the flow vis-à-vis the phenomenon of cavitation. The results showed that as the number of stator blades increases, the dimension of the cavitation bubbles widens and intensifies for 6 stator blades.

On the other hand, the results also showed that as the number of rotor blades increases, the cavitation pocket increases, especially at the tip of the blade on the upper surface approaching the edge of attack. Finally, if we combine the results of the cavitating and non-cavitating flow, we can retain the configuration (NS = 5, NR = 6), since it presents both better efficiency and power with a very minimal appearance of a cavitation of the order of  $10^{-6}$ .

## REFERENCES

- [1] S.Q. Cai: Cavitation occurring in capillary tubes. *Phys. Lett.* **383** (6) (2019). Available from: <https://doi.org/10.1016/j.physleta.2018.11.026>.
- [2] X.W. Luo, T. Ji, T. Tsujimoto: A review of cavitation in hydraulic machinery. *J. Hydrodyn.* **28** (3) (2016). Available from: [https://doi.org/10.1016/S1001-6058\(16\)60638-8](https://doi.org/10.1016/S1001-6058(16)60638-8).
- [3] C. Luis, O. Eduardo, D. Marcelo, C. P. Antonio: Assessment of turbulence modeling for CFD simulation into hydroturbines : spiral casings. In: *17th International Mechanical Engineering Congress (COBEM2003)*, Sao Paulo, Brazil (2003). Available from: <https://abcm.org.br/anais/cobem/2003/html/pdf/COB03-0843.pdf>.
- [4] A. Gehrler, H. Benigni, M. Kostenberger: Unsteady simulation of the flow through a horizontal-shaft bulb turbine. In: *22nd IAHR Symposium on Hydraulic Machinery and Systems*, Stockholm, Sweden (2004). Available from: <https://www.researchgate.net/publication/239548676>.
- [5] C.C.B. Santos, J. G. Coelho, A. C. P. Brasil Junior: Numerical study of a bulb hydraulic turbine. In: *12th International Symposium on Transport Phenomena and Dynamics of Rotating Machinery*, Honolulu, Hawaii (2008). Available from: <https://www.abcm.org.br/anais/cobem/2007/pdf/COBEM2007-2241.pdf>.
- [6] H. Begnigni, H. Jaberg: Stationary and transient numerical simulation of a bulb turbine. In: *Proceeding of the 5th IASME/WSEAS International Conference on Fluid Mechanics and Aerodynamics*, (FMA 2007), Vouliagmeni Beach, Athens, Greece (2007). Available from: <https://www.researchgate.net/publication/228416629>.
- [7] R.O. Edwin: Analyse de l'écoulement dans la roue d'une turbine hydraulique axiale de type hélice : prise en considération du jeu de bout d'aube. Thèse de Master, Université Laval, Quebec (1998). Available from: <https://hdl.handle.net/20.500.11794/22604>.
- [8] H. Nilsson, L. Davidson: A numerical investigation of tip clearance flow in Kaplan water turbines. In: *Proceedings of Hydropower into the Next Century-III*, Gmunden, Austria (1999). Available from: [https://www.cfd-sweden.se/lada/postscript\\_files/haakan\\_paper.pdf](https://www.cfd-sweden.se/lada/postscript_files/haakan_paper.pdf).
- [9] E. Ayli: Cavitation in hydraulic turbines. *Heat Technol.* **37** (1) (2019). Available from: <https://doi.org/10.18280/ijht.370140>.
- [10] M. Grekula, G. Bark: Experimental study of cavitation in a Kaplan model turbine. In: *Fourth International Symposium on Cavitation (CAV 2001)*, California Institute of Technology (Caltech), Pasadena, California (2001). Available from: <https://web.archive.org/web/20150911004236/http://caltechconf.library.caltech.edu/73/1/cav2001.pdf>.